# Control of Aggregate Air-Conditioning Load using Packetized Energy Concepts

Oluwagbemileke Oyefeso, Gregory S. Ledva, Mads Almassalkhi, Ian A. Hiskens, and Johanna L. Mathieu

*Abstract*— **The paper extends the packetized energy management (PEM) control strategy to enable coordination of compressor-based thermostatically controlled loads (TCLs), such as air conditioners. This establishes a new method of harnessing the flexibility of this ubiquitous resource, enabling a variety of grid services, such as frequency regulation. In the original PEM scheme, resources request energy packets and turn on if their request is approved. That PEM scheme has been further extended by introducing the concept of turn-off requests. We find that this increases flexibility and improves tracking performance. Through a case study involving over 1000 air conditioners, we evaluate the performance of a population of TCLs providing frequency regulation under PEM, highlighting both the capabilities and limitations. Simulations indicate our controller extensions significantly increase resource availability and tracking performance. We show that it is possible to achieve RMS tracking error below 2% when providing more than 250 kW of frequency regulation.**

## Nomenclature

| | |
|---|---|
| $C_{\mathrm{a}}$ | Air thermal mass [kWh/°C]. |
| $C_{\mathrm{m}}$ | Building thermal mass [kWh/°C]. |
| $H_{\mathrm{m}}$ | Conductance between inner air & solid mass [kW/(°C)]. |
| $k$ | Time step [-]. |
| $\mathscr{K}_{\mathrm{lock}}$ | Set of lock-out time-steps [-]. |
| $m$ | ON/OFF switching variable [-]. |
| $M_{\mathrm{on}}$ | Mean on-request frequency [Hz]. |
| $M_{\mathrm{off}}$ | Mean off-request frequency [Hz]. |
| $n$ | Air Conditioner index [-]. |
| $Q_{\mathrm{a}}$ | Heat flux into interior mass [kW]. |
| $Q_{\mathrm{m}}$ | Heat flux into interior solid mass [kW]. |
| $R_n^{\mathrm{on}}$ | Energy packet request [-]. |
| $R_n^{\mathrm{off}}$ | Turn-off request [-]. |
| $t^{\mathrm{on}}$ | Epoch [s]. |
| $t_{\mathrm{locked}}^{\mathrm{on}}$ | Compressor turn-on lock-out time [s]. |
| $t_{\mathrm{locked}}^{\mathrm{off}}$ | Compressor turn-off lock-out time [s]. |
| $t_{\mathrm{min}}^{\mathrm{on}}$ | Energy packet minimum epoch length [s]. |
| $t_{\mathrm{max}}^{\mathrm{on}}$ | Energy packet maximum epoch length [s]. |
| $t_{\mathrm{comp}}$ | Compressor lock-out timer [s]. |
| $t_n$ | Elapsed epoch time for AC $n$ [s]. |
| $T_{\mathrm{a}}$ | Indoor Air Temperature [°C]. |
| $T_{\mathrm{m}}$ | Inner Mass Temperature [°C]. |
| $T_{\mathrm{o}}$ | Outdoor Air Temperature [°C]. |
| $T_n^{\mathrm{set}}$ | Temperature set-point [°C]. |
| $T_n^{\mathrm{min}}$ | Lower dead-band temperature [°C]. |
| $T_n^{\mathrm{max}}$ | Upper dead-band temperature [°C]. |
| $U_{\mathrm{a}}$ | Conductance of building envelope [kW/°C]. |
| $\Delta t$ | Time step duration [s]. |
| $\mu$ | Temperature based rate parameter [-]. |
| $\gamma$ | Time based rate parameter [-]. |

## I. Introduction

Environmental concerns and the drive to decarbonize the power sector have resulted in traditional generation, such as coal fired power plants, being phased out and replaced by renewable energy alternatives. Continual growth in renewable generation requires an increase in the amount of balancing services needed to compensate for the inherently intermittent nature of renewable energy generation and maintain power grid reliability [1]. Traditionally, balancing services have been provided by synchronous generators, but new sources of flexibility are needed. Aggregations of distributed energy resources (DERs) such as thermostatically controlled loads (TCLs), and more specifically residential air conditioners (ACs), can offer such flexibility [2]–[8].

The recent US Federal Energy Regulatory Commission Order 2222 [9] requires that grid operators revise their rules to enable DER aggregations to participate alongside other traditional resources in wholesale markets. This signals a paradigm shift in electricity markets that will lead to increased participation of DERs, such as flexible load aggregations. It ensures the need for load coordination and control strategies that meet both technical requirements and market participation criteria, and readily scale from the literature to real-world applications.

Houses have thermal inertia which allows ACs the flexibility to shift their energy consumption in time. Furthermore, ACs are ubiquitous resulting in a large resource potential;

This work was supported by the U.S. Department of Energy's Advanced Research Project Agency - Energy (ARPA-E), Award DE-AR0001061. M. Almassalkhi was supported by ARPA-E award DE-AR0000694 and is co-founder of startup Packetized Energy, which is actively commercializing Packetized Energy Management. O. Oyefeso, I.A. Hiskens, and J.L. Mathieu are with the Department of Electrical Engineering and Computer Science, University of Michigan, Ann Arbor, MI, USA {ooyefeso, jlmath, hiskens}@umich.edu. M. Almassalkhi is with the Department of Electrical and Biomedical Engineering, University of Vermont, Burlington, VT, USA malmassa@uvm.edu. G.S. Ledva is with Virtual Peaker gledva@virtual-peaker.com.

almost 90% of US homes utilize air conditioning equipment [10]. Usage of residential ACs is also common in other countries [3], [11], [12]. The abundant and distributed geographic location of ACs make them prime and valuable candidates for providing flexibility to the grid, especially when aggregated.

Leveraging these AC resources for grid services requires coordination and control that is non-disruptive to occupants, robust, dynamic, and efficient, whilst satisfying concerns for privacy and autonomy. Numerous AC coordination and control schemes have been proposed. Some are centralized, others decentralized, some are model free, others model based, some are suitable for fast time scale dynamic signals, others can only work on slower time scales [5], [13]–[20]. However, there remains scope for improving effectiveness and practicality.

The goal of this paper is to develop a packetized energy management (PEM) approach [21] to effectively control an aggregation of ACs to provide frequency regulation. PEM is a device-focused scheme that has been shown in a real-world application to achieve non-disruptive, asynchronous, and anonymous load coordination using electric resistance water heaters for load following, i.e., tracking a reference signal over an extended period (4 hours). However, the existing PEM scheme does not explicitly consider the capabilities and constraints of compressor-based TCLs like ACs, heat pumps, and refrigerators, which exhibit fundamentally different dynamics to resistance-based TCLs. Moreover, resistance-based TCLs (water and space heaters) are gradually being replaced by compressor-based TCLs because they are more efficient. Hence, there is a need to extend the PEM scheme to cater for compressor-based TCLs.

A significant amount of work has been undertaken on the PEM control scheme. A macro-model was developed in [22] for a homogeneous population of electric water heaters under PEM control. This macro-model was extended in [23] to a diverse group consisting of electric water heaters and energy storage systems operating under PEM. Analysis in [24] provided a discrete-time control law that maximizes requests accepted whilst tracking a regulation signal. This analysis is further extended in [25], [26] to accommodate diverse device types, including batteries, EVs, and resistance-based water heaters. Finally, [27] develops a decentralized frequency-responsive control scheme for electric water heaters, using local frequency-dependent control policies based on an adaptation of PEM. However, none of this prior work has considered ACs with operational compressor constraints.

In this paper, we develop a non-disruptive control approach to coordinate ACs under PEM, with the goal of allowing an aggregator to provide frequency regulation. Our approach accounts for compressor lock-out, i.e., compressors cannot be switched on immediately after switching off or switched off immediately after switching on. This restriction has been considered in other load control work, e.g., [28], but not PEM. We also improve capabilities of the PEM scheme by incorporating turn-off mechanisms, i.e., TCLs not only issue a request to turn on but can also request to turn off.

The paper makes a number of contributions. First, we adapt the PEM control strategy to compressor-based cooling TCLs and introduce the idea of a flexible epoch (the duration of time for which the TCL is turned on). This mitigates the negative effect of lock-out on resource availability. Second, we extend the PEM control strategy to incorporate a mechanism for turning TCLs off mid-epoch, which increases flexibility and improves tracking performance. Third, we demonstrate PEM for compressor-based TCLs under realistic conditions, showing significant improvements in the fleet's performance score.

The paper is structured as follows. Section II describes AC operation and our AC model, provides an overview of PEM, and proposes a modification to PEM that allows compressor-based loads, such as ACs, to be incorporated. Section III details the controller modifications needed to support turn-off requests. Case study results and analysis are presented in Section IV, while Section V provides concluding remarks and discusses future directions.

## II. Air Conditioner Control with PEM

### A. AC Overview and Model

AC power consumption is determined by its ON/OFF state, which is governed by a thermostat. The thermostat utilizes a temperature dead-band $[T^{\min}, T^{\max}]$ to achieve hysteretic control that regulates temperature around a set-point $T^{\text{set}}$. The dead-band confines the house temperature to a narrow comfort region around the set-point. For fixed power ACs, i.e., ACs that consume rated power when cooling and minimal power when not, a dead-band is necessary to prevent the AC from frequent cycling, which would lead to wear-and-tear and shorten its lifespan. The AC turns on (cools) when the temperature rises to $T^{\max}$, remains on until the temperature falls to $T^{\min}$, then switches off until the temperature rises again to $T^{\max}$. This cycle gives rise to alternating periods of rated power draw and little/no power draw. Fixed power ACs are dominant in the US.

We model ACs using the equivalent thermal parameter (ETP) model of [29]–[34], with indoor air temperature $T_{\text{a}}$ and inner mass temperature $T_{\text{m}}$ dynamics given by,

$$\begin{aligned}\dot{T}_{\text{a}}(t) &= \frac{1}{C_{\text{a}}}(T_{\text{m}}(t)H_{\text{m}} - (U_{\text{a}}+H_{\text{m}})T_{\text{a}}(t) + Q_{\text{a}}(m(t)) \\ &\qquad + T_{\text{o}}(t)U_{\text{a}}), \\ \dot{T}_{\text{m}}(t) &= \frac{1}{C_{\text{m}}}\left(H_{\text{m}}(T_{\text{a}}(t) - T_{\text{m}}(t)) + Q_{\text{m}}\right),\end{aligned}$$

where $C_{\text{a}}$ is the air thermal mass, $H_{\text{m}}$ is the conductance between inner air and solid mass, $U_{\text{a}}$ is the conductance of the building envelope, $T_{\text{o}}$ is the outdoor air temperature, $C_{\text{m}}$ is the building thermal mass, and $Q_{\text{m}}$ is the heat flux to the interior solid mass. Function $Q_{\text{a}}$ is the heat flux into the interior mass, which includes the internal and ambient heat gains and cooling from the AC, which in turn is a function of the AC's discrete on/off mode $m$. These dynamics can be expressed as a linear time-invariant system

$$\dot{x}(t) = Ax(t) + Bu(t),$$

where

$$x(t) = \begin{bmatrix} T_\text{a}(t) & T_\text{m}(t) \end{bmatrix}^T,$$
$$u(t) = \begin{bmatrix} Q_\text{a}(m(t)) & T_\text{o}(t) & Q_\text{m} \end{bmatrix}^T,$$
$$A = \begin{bmatrix} -(U_\text{a}+H_\text{m})/C_\text{a} & H_\text{m}/C_\text{a} \\ H_\text{m}/C_\text{m} & -H_\text{m}/C_\text{m} \end{bmatrix},$$
$$B = \begin{bmatrix} 1/C_\text{a} & U_\text{a}/C_\text{a} & 0 \\ 0 & 0 & 1/C_\text{m} \end{bmatrix}.$$

Using a timestep of $\tau$, the above continuous-time state space model can be discretized as,

$$x[k+1] = A_d x[k] + B_d u[k],$$

where $A_d = e^{A\tau}$ and $B_d = A^{-1}(A_d - I)B$.

In discrete time, the on/off switching dynamics are,

$$m[k+1] = \begin{cases} 1, & \text{if } m[k] = 0 \ \wedge \ T_\text{a}[k] \geq T^\text{max} \\ 0, & \text{if } m[k] = 1 \ \wedge \ T_\text{a}[k] \leq T^\text{min} \\ m[k], & \text{otherwise.} \end{cases}$$

AC manufacturers also include compressor lock-out restrictions. After an AC has turned on it cannot turn off for a duration of $t^\text{on}_\text{locked}$ and after it has turned off it cannot turn on for a duration of $t^\text{off}_\text{locked}$. The lock-out times prevent the compressor from rapidly oscillating between states, protecting it from short cycling, and prolonging its lifespan.

### B. Packetized Energy Management Overview

In PEM, TCLs make a request to turn on for fixed-duration periods to consume a fixed amount of energy. This has the effect of splitting and shifting their consumption in time such that they are on for shorter durations and switched more often. The concept is motivated by digital communications where large data packets are broken and transmitted in smaller packets. The fixed-duration energy consumption is referred to as an *energy packet*. The fixed duration is called the *epoch*, $t^\text{on}$. TCLs choose whether to request an energy packet based on their air temperature and on/off state. The load aggregator coordinating the TCLs approves or denies the energy packet requests to achieve some overarching objective, such as using the aggregate power consumption of the TCLs to track a reference signal [21], [25], [26].

Fig. 1 shows the PEM scheme for TCLs. In this diagram, we see that the *Packetized Energy Controller* at the device in the consumer's home contains *Request Logic* that determines when the TCL should request an energy packet. This request logic utilizes local state information from TCLs to decide whether or not to make an *Energy Packet Request*. The aggregator processes the requests along with the *Desired Aggregate Power* of the fleet and uses its *Request Processing Logic* to decide whether to approve or deny each packet request. Since energy requests are initiated by the TCLs, they arrive stochastically at the aggregator. The requests are anonymous, i.e., the identity of requesting TCLs is encrypted and unavailable to the aggregator, thus preserving consumer privacy. The aggregator accepts/denies requests based on system needs. This overall process ensures fair resource deployment.

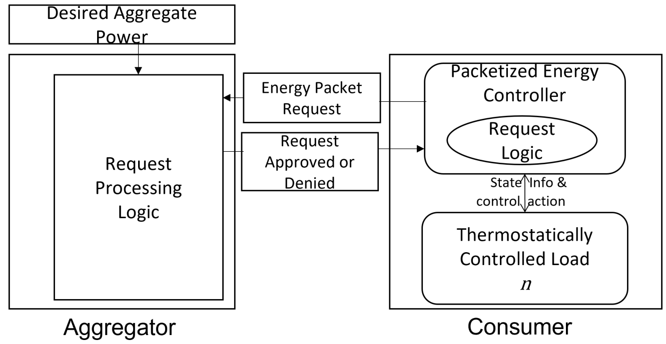


Fig. 1. PEM Scheme for TCLs.

TCLs participating in PEM make energy requests automatically and probabilistically. Specifically, we adopt the approach from [21], where the probability that AC $n$ makes an energy packet request $R^\text{on}_n$ during the $k$th time-step (of duration $\Delta t$) is computed with the cumulative exponential distribution function,

$$P(R^\text{on}_n | T_{\text{a},n}[k]) := 1 - e^{-\mu(T_{\text{a},n}[k])\Delta t}, \tag{1}$$

where $T_{\text{a},n}$ is the indoor air temperature of the house conditioned by AC $n$ and $\mu(T_{\text{a},n}[k])$ is a rate parameter based on the indoor air temperature (and defined below). We also take into account the AC's temperature dead-band to force an energy packet request if the house temperature is at the upper dead-band limit and ensure there is no request if the temperature is at the lower dead-band limit, i.e.,

$$P(R^\text{on}_n \mid T_{\text{a},n}[k] \leq T^\text{min}_n) = 0, \tag{2}$$
$$P(R^\text{on}_n \mid T_{\text{a},n}[k] \geq T^\text{max}_n) = 1. \tag{3}$$

However, to ensure consumer comfort is always satisfied, the TCL reverts to default thermostat control when outside the dead-band, i.e., when $T_{\text{a},n}[k] > T^\text{max}_n$ the AC does not make an energy packet request but simply turns on.

The rate parameter is defined as,

$$\mu(T_{\text{a},n}[k]) = \begin{cases} 0, & \text{if } T_{\text{a},n}[k] \leq T^\text{min}_n \\ f(T_{\text{a},n}), & \text{if } T_{\text{a},n}[k] \in (T^\text{min}_n, T^\text{max}_n) \\ \infty, & \text{if } T_{\text{a},n}[k] \geq T^\text{max}_n \end{cases} \tag{4}$$

where

$$f(T_{\text{a},n}[k]) = \left( \frac{T_{\text{a},n}[k] - T^\text{min}_n}{T^\text{max}_n - T_{\text{a},n}[k]} \right) M_\text{on} \tag{5}$$

and $M_\text{on}$ is the mean on-request frequency at $T_{\text{a},n}[k] = T^\text{set}_n := (T^\text{max}_n + T^\text{min}_n)/2$, which is a design parameter. A mean time to on-request of 10 min implies $M_\text{on} = \frac{1}{600}$ Hz [21]. We slightly constrict the dead-band limits used within (2)–(5), creating a PEM dead-band, to help prevent violation of the true TCL dead-band constraints. This is particularly important for TCLs that change status close to the dead-band limits and that are required to remain in their new status for a fixed duration [21]. The choice of constriction is a design choice based on the thermal dynamics and epoch duration.

### C. Air Conditioners as a Packetized Load

The PEM scheme presented in Section II-B does not address compressor lock-out. We next describe a modification to PEM that caters for compressor-based loads. The controller is equipped with a timer $t_{\text{comp}}$, which turns on whenever the compressor changes status, and resets to zero at the conclusion of the relevant lock-out period. Specifically, over the lock-out period following AC turn on, $t_{\text{comp}} \in (0, t^{\text{on}}_{\text{locked}}]$, with $t_{\text{comp}}$ resetting after $t^{\text{on}}_{\text{locked}}$. Likewise, over the lock-out period following AC turn off, $t_{\text{comp}} \in (0, t^{\text{off}}_{\text{locked}}]$ and resets after $t^{\text{off}}_{\text{locked}}$. We refer to the set of timesteps during which the AC is off and locked as $\mathscr{K}^{\text{off}}_{\text{lock}}$ and those when the AC is on and locked as $\mathscr{K}^{\text{on}}_{\text{lock}}$. The AC makes no PEM requests when locked, i.e., (1) is overridden by $P(R^{\text{on}}_n | T_{\text{a},n}[k]) := 0$ when $t_{\text{comp}} > 0$, and (2)-(3) are replaced by,

$$P\big(R^{\text{on}}_n | T_{\text{a},n}[k] \le T^{\min}_n \vee k \in \mathscr{K}^{\text{off}}_{\text{lock}} \vee k \in \mathscr{K}^{\text{on}}_{\text{lock}}\big) = 0, \quad (6)$$

$$P\big(R^{\text{on}}_n | T_{\text{a},n}[k] \ge T^{\max}_n \wedge k \notin \mathscr{K}^{\text{on}}_{\text{lock}} \wedge k \notin \mathscr{K}^{\text{off}}_{\text{lock}}\big) = 1. \quad (7)$$

Note that the epoch must be chosen to be larger than the on lock-out time, $t^{\text{on}} > t^{\text{on}}_{\text{locked}}$. Otherwise, at the end of an epoch when the TCL was due to turn off, it would be prevented from doing so by the lock-out override, and would revert to default thermostat control.

ACs that are able to make PEM requests, i.e., operating within the PEM dead-band and not locked, are considered available. Compressor lock-out significantly reduces TCL availability as we will demonstrate through case studies in Section IV-B. Reduced availability impacts control performance, which motivates the controller extensions in the following section.

## III. Controller Extensions

In the PEM scheme presented in the previous section, the aggregator has the ability to turn on TCLs (by approving energy packet requests) but cannot turn off TCLs should the need arise. This makes it hard to closely track downward trajectories of the reference signal, as the aggregator must rely solely on rejecting all new energy packet requests and waiting for the unforced reduction in aggregate power consumption as AC epochs expire. This issue is compounded by compressor lock-out, which reduces TCL availability since TCLs are locked and unavailable as soon as they switch off at the end of an epoch. Reduced availability makes it harder to track in general. We will illustrate the impact of these limitations through case studies in Section IV-B.

To mitigate the effects of these practical challenges, we introduce a flexible epoch and a turn-off mechanism that increase flexibility and TCL availability. The epoch length $t^{\text{on}}$ now lies in the range $[t^{\text{on}}_{\min}, t^{\text{on}}_{\max}]$ where $0 < t^{\text{on}}_{\text{locked}} \le t^{\text{on}}_{\min} \le t^{\text{on}}_{\max}$. The controller is equipped with a timer that records the elapsed epoch duration of an energy packet, $t \in (0, t^{\text{on}}_{\max}]$. An AC with an accepted energy packet request will turn on for an epoch length that is at least $t^{\text{on}}_{\min}$ and no greater than $t^{\text{on}}_{\max}$.

The turn-off mechanism enables turn-off requests $R^{\text{off}}_n$ during the epoch range $(t^{\text{on}}_{\min}, t^{\text{on}}_{\max}]$. The probability that AC

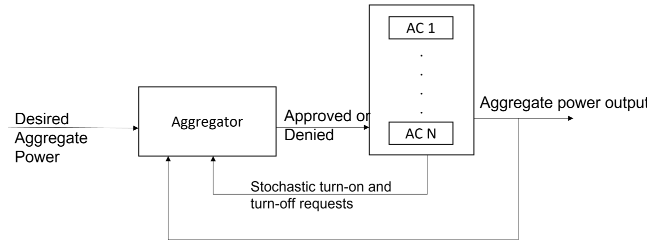


Fig. 2. Extended PEM for closed-loop control of an AC aggregation.

$n$ in the ON state, operating in the PEM scheme, having an elapsed epoch time of $t_n \in (0,\ t^{\text{on}}_{\max}]$, makes a turn-off request $R^{\text{off}}_n$ during the $k$th time-step is,

$$P\big(R^{\text{off}}_n | T_{\text{a},n}[k], t_n[k]\big) := \big(1 - e^{-\mu^{\text{off}}(T_{\text{a},n}[k])\Delta t}\big)\big(1 - e^{-\gamma(t_n[k])\Delta t}\big), \quad (8)$$

where the turn-off temperature-based rate parameter is,

$$\mu^{\text{off}}(T_{\text{a},n}[k]) = \begin{cases} 0, & \text{if } T_{\text{a},n}[k] \ge T^{\max}_n \\ \left(\frac{T^{\max}_n - T_{\text{a},n}[k]}{T_{\text{a},n}[k] - T^{\min}_n}\right) M_{\text{off}}, & \text{if } T_{\text{a},n}[k] \in (T^{\min}_n, T^{\max}_n) \\ \infty, & \text{if } T_{\text{a},n}[k] \le T^{\min}_n \end{cases} \quad (9)$$

the time-based rate parameter is,

$$\gamma(t_n[k]) = \begin{cases} 0, & \text{if } t_n[k] \le t^{\text{on}}_{\min} \\ \left(\frac{t_n[k] - t^{\text{on}}_{\min}}{t^{\text{on}}_{\max} - t_n[k]}\right) M_{\text{off}}, & \text{if } t_n[k] \in (t^{\text{on}}_{\min}, t^{\text{on}}_{\max}) \\ \infty, & \text{if } t_n[k] \ge t^{\text{on}}_{\max} \end{cases} \quad (10)$$

and $M_{\text{off}}$ is the mean off-request frequency, a design parameter similar to $M_{\text{on}}$ described in Section II and detailed in [21]. Then the turn-off request is constrained as,

$$P\big(R^{\text{off}}_n | T_{\text{a},n}[k] \le T^{\min}_n \wedge t_n[k] \ge t^{\text{on}}_{\max} \wedge k \notin \mathscr{K}^{\text{on}}_{\text{lock}} \wedge k \notin \mathscr{K}^{\text{off}}_{\text{lock}}\big) = 1, \quad (11)$$

$$P\big(R^{\text{off}}_n | T_{\text{a},n}[k] \ge T^{\max}_n \vee t_n[k] \le t^{\text{on}}_{\min} \vee k \in \mathscr{K}^{\text{on}}_{\text{lock}} \vee k \in \mathscr{K}^{\text{off}}_{\text{lock}}\big) = 0. \quad (12)$$

To ensure consumer comfort, the TCL reverts to default thermostat control and does not make turn-off requests when outside the temperature dead-band, similar to Section II-B. It also does not make turn-off requests when the AC is locked. The turn-off mechanism is consistent with the distributed nature of the PEM algorithm with request probabilities computed locally. Equation (9) ensures TCLs closer to the lower dead-band temperature have higher probabilities of making turn-off requests and (10) enables TCLs with higher elapsed epoch duration to have higher probabilities of making turn-off requests.

Fig. 2 shows the closed loop feedback system for a load aggregator with ACs under PEM control. The load aggregator receives a reference signal from the grid operator and must then coordinate the available resources to match that signal. Thus, at each sample period $k$, the load aggregator has two queues of anonymous energy packet requests (henceforth referred to as turn-on requests) and anonymous turn-off requests from ACs under its control. If the aggregate power consumption of the AC population under the load aggregator's control under- or over-shoots the reference signal, the aggregator first determines the number of turn-on or turn-off requests, respectively, to approve to minimize the tracking error. This is achieved by dividing the tracking error by an estimate of the average AC power consumption. The aggregator then selects and approves the desired number of ON/OFF requests from the corresponding queue. All other requests are denied.

The fixed epoch design of the original PEM scheme means that devices with approved packet requests are effectively unavailable as they cannot make further PEM requests during the epoch duration. The flexible epoch and turn-off mechanism allows these devices to become available for control once they have met their minimum epoch time. Because they can start making PEM turn-off requests, overall TCL availability is increased. This in turn improves the range of corrective actions (flexibility) and tracking performance as the aggregator has access to more requests. Also, the turn-off requests provide the aggregator with the ability to actively track downward reference trajectories. Specifically, in addition to rejecting new turn-on requests and the unforced reduction in aggregate power consumption due to epochs expiring, the aggregator can now actively turn off ACs mid epoch. The benefits of this new approach are demonstrated through the following case studies.

## IV. Case Studies

### A. Simulation Scenarios and Parameters

The case studies consider the response of 1103 ACs that are controlled using the PEM scheme to provide frequency regulation. The parameters of the ACs were generated using GridLAB-D [29], with ±10% random variation around each parameter. Each AC consumes 2.5 kW on average. This study considers houses with single central AC units, but is directly applicable and extendable to houses with multiple AC units given that every AC unit will make its own PEM request. The PJM RegD signal [35] was used as the reference signal to be tracked. Table I lists the simulation parameters that were used. As explained in Section II-B, we constrict the dead-band used by the PEM controller, referred to as the PEM dead-band. Here we set the PEM dead-band width to $0.8(T_n^{\max} - T_n^{\min})$ for all ACs, where 0.8 is a design choice that has been found to sufficiently mitigate violations of the AC thermostat dead-bands.

We assess the AC population's tracking performance under a variety of conditions. Specifically, we define seven cases with varying amounts of regulation capacity, with and without the controller extensions (flexible epoch and turn-off capability), and with and without compressor lock-out.

### B. Simulation Results

Table II and Fig. 3 summarize the controller performance results across all of the cases. Table II gives the normalized root mean square error (NRMSE) between the aggregate power and the power reference, normalized by the baseline power consumption of the aggregation. We also provide an industry performance metric, namely PJM performance scores [36], and the mean availability, which is calculated as the average percentage of available devices over the simulation period. An AC is considered available when it is unlocked and within the PEM temperature dead-band, and hence available to participate and make turn-on or turn-off requests under the PEM scheme. The top set of plots in Fig. 3 show the reference signal that is to be tracked, the aggregate power of the ACs, and the baseline power consumption. The bottom set of plots show the percentage of available ACs, the ramp-up flexibility, and the ramp-down flexibility. The ramp-up/down flexibility is the fraction of available ACs making turn-on/off requests. It defines the flexibility the aggregator has in increasing/decreasing aggregate power consumption by approving turn-on/off requests.

TABLE I
Simulation Parameters

| Parameters | Value | Parameters | Value |
|---|---|---|---|
| $\Delta t$ | 2 s | $t^{\text{on}}$ | 10 min |
| $t^{\text{on}}_{\text{locked}}$ | 3 min | $t^{\text{off}}_{\text{locked}}$ | 5 min |
| $t^{\text{on}}_{\min}$ | 3 min | $t^{\text{on}}_{\max}$ | 10 min |
| $T_n^{\text{set}}$ | $[20,24]$°C | $T_n^{\max} - T_n^{\min}$ | $[1,2]$°C |
| $T_{\text{o}}$ | 32.22°C | $M_{\text{off}}$ | 1 Hz |
| $M_{\text{on}}$ | $\frac{1}{300}$ Hz | Simulation Period | 1 h |

Fig. 4 shows the fraction of the population that is ON/OFF and the portion of those that are available/unavailable for Cases 0–2. Table III presents these values averaged over the simulation period. By comparing the results of Cases 0 and 1, we can see the impact of compressor lock-out on availability, which in turn affects performance. We see in Case 0 that an average of 55.8% ACs are ON while the remaining 44.2% are OFF and available because lock-out is ignored in Case 0. In Case 1, an average of 54.3% of ACs are ON, but of the 45.7% that are OFF, only 18.9% are available because of compressor lock-out. Hence, lock-out reduces the mean AC availability by a factor of 134%. This disparity in availability accounts for the noticeable difference in the ramp-up flexibility between both cases (shown in Fig. 3) as there are fewer available ACs making requests. Due to the reduced flexibility, we see from Table II that the PJM composite score decreases from 0.87 to 0.85 and the NRMSE increases from 5.45% to 5.59%. This effect becomes more pronounced when regulation capacity increases.

By comparing the results of Cases 1 and 2, we see that the extended controller mitigates the influence of lock-out on availability. We see from Table III that this results in an improvement of the mean device availability by a factor of 293%, which in turn affects the ramp-up/down flexibility, as seen in Fig. 3. This improved flexibility yields an increase in PJM composite performance score from 0.85 to 0.96 and a decrease in NRMSE from 5.59% to 1.62%. Fig. 5 highlights a 15 min window of the tracking results shown in Fig. 3 for Cases 1 and 2, clearly showing the impact of the controller extension on tracking performance.

Comparing the results of Cases 1–2, Cases 3–4, and Cases 5–6, we see that the controller extensions greatly increase device availability and flexibility. In Fig. 3, we see

TABLE II

CONTROLLER PERFORMANCE RESULTS ACROSS ALL CASES

| | Case 0 | Case 1 | Case 2 | Case 3 | Case 4 | Case 5 | Case 6 |
|---|---|---|---|---|---|---|---|
| Regulation Capacity (MW) | 0.25 | 0.25 | 0.25 | 0.5 | 0.5 | 1 | 1 |
| Flexible Epoch and Turn-off Capability | No | No | Yes | No | Yes | No | Yes |
| Compressor Lock-out | No | Yes | Yes | Yes | Yes | Yes | Yes |
| NRMSE (%) | 5.45 | 5.59 | 1.62 | 15.11 | 12.50 | 36.01 | 35.29 |
| PJM Accuracy Score (0-1) | 0.88 | 0.87 | 0.99 | 0.80 | 0.92 | 0.76 | 0.79 |
| PJM Delay Score (0-1) | 0.98 | 0.97 | 1.00 | 0.94 | 0.98 | 0.93 | 0.95 |
| PJM Precision Score (0-1) | 0.73 | 0.70 | 0.88 | 0.55 | 0.77 | 0.39 | 0.62 |
| PJM Composite Score (0-1) | 0.87 | 0.85 | 0.96 | 0.77 | 0.89 | 0.69 | 0.78 |
| Mean Availability (%) | 44.17 | 18.88 | 74.18 | 19.03 | 61.14 | 18.87 | 47.68 |

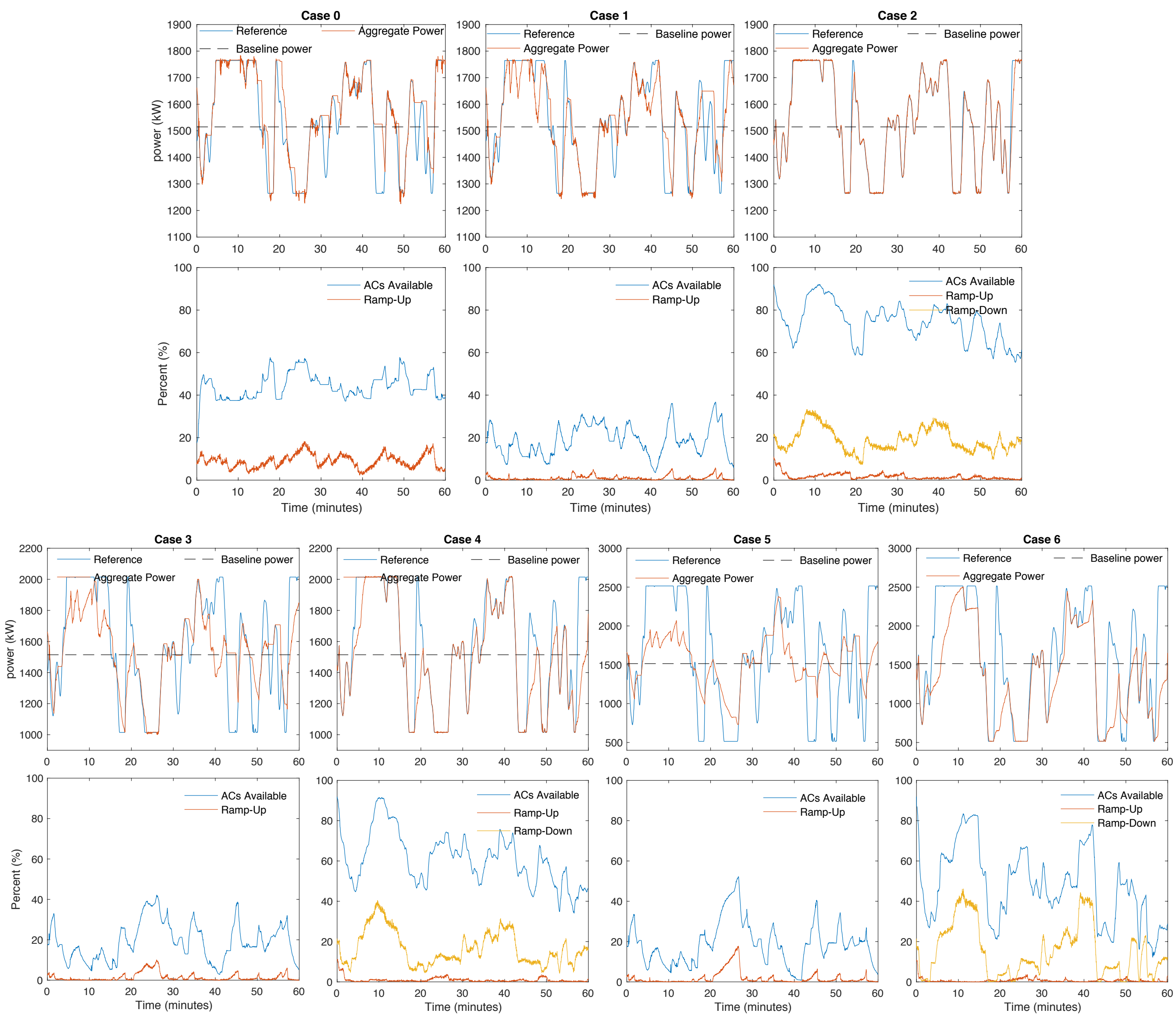


Fig. 3. Reference tracking, resource availability, and flexibility for all cases.

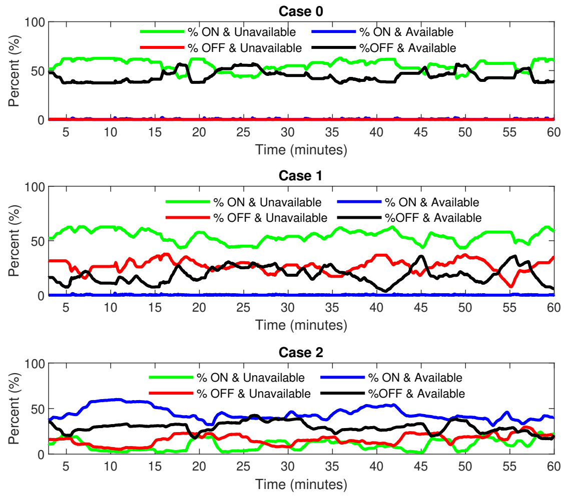


Fig. 4. Effect of lock-out and controller extensions on AC availability.

TABLE III
AVERAGE AC AVAILABILITY

| | Case 0 | Case 1 | Case 2 |
|---|---|---|---|
| ACs ON (%) | 55.8 | 54.3 | 54.2 |
| ACs OFF (%) | 44.2 | 45.7 | 45.8 |
| ON & Unavailable (%) | 55.8 | 54.3 | 10.0 |
| ON & Available (%) | 0 | 0 | 44.2 |
| OFF & Unavailable (%) | 0 | 26.8 | 15.9 |
| OFF & Available (%) | 44.2 | 18.9 | 30.0 |

instances where the standard PEM controller is unable to track an upward trajectory as it is limited by the available ACs and ramp-up flexibility, and also unable to actively track downward trajectories without the turn-off mechanism. For example, comparing Cases 3 and 4, we see from Table II that the NRMSE decreases from 15.11% to 12.50%, mean device availability increases by a factor of 221.3%, and the PJM composite score increases from 0.77 to 0.89. Comparing Cases 5 and 6, we see a decrease in NRMSE from 36.01% to 35.29%, an increase in mean device availability by a factor of 152.7%, and an increase in the PJM composite score from 0.69 to 0.78.

PJM requires composite scores greater than 0.75 [36] and we see that the extended PEM controller qualifies for market participation with 0.25, 0.5, or 1 MW of regulation capacity. The original controller falls short in the 1 MW scenario (Case 5) because of the limited number of ACs. From Fig. 3 we see the tracking is often hampered by the available ramp-up and ramp-down capacity. More devices are simply needed.

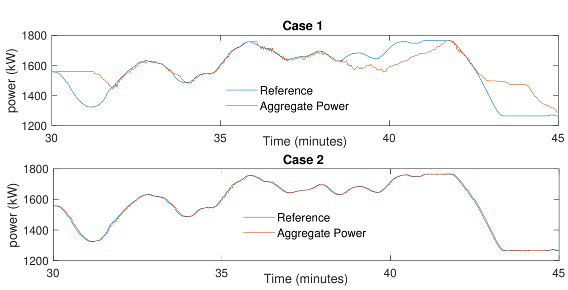


Fig. 5. Close-up of the tracking results for Cases 1 and 2.

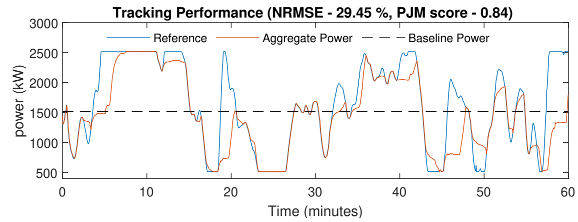


Fig. 6. Extended PEM providing 1 MW frequency regulation, with new $M_{\text{on}}$. PJM composite score is 0.84.

To improve the performance in the 1 MW frequency regulation capacity case, we adjusted $M_{\text{on}}$ to increase the turn-on request rate while holding all other parameters constant. This increases the number of ACs available to the aggregator. Fig. 6 shows the new tracking performance; the PJM composite score increases from 0.78 (Case 6 in Table II) to 0.84. Performance is limited and constrained by the number of available ACs. Accordingly, it is important to be able to ascertain the number of ACs needed to offer a given regulation capacity or the maximum capacity attainable by a given population of ACs, along with the corresponding optimal parameters, whilst taking into account the required performance objectives. Estimating the flexibility and choosing the optimal parameters heuristically via multiple simulations is cumbersome and inefficient due to the large parameter space [37]. Hence, developing an aggregate model that accurately approximates the dynamics of compressor-based TCLs is a future research direction. The flexibility and optimal parameter selection is impacted by ambient conditions. For example, the flexibility under nominal conditions will differ significantly from that under extreme heat conditions when most ACs will be constantly ON. We will address performance, flexibility, and optimal parameter selection under extreme conditions in future work.

## V. CONCLUSION

In this paper, we extended the PEM aggregate control scheme to incorporate compressor-based TCLs. We included compressor lock-out constraints and developed both flexible epochs and a turn-off mechanism. We showed that these extensions improve device availability, flexibility, and controller performance. We found that with a population of around 1000 ACs, it is possible to offer up to 1 MW of frequency regulation capacity while meeting PJM market qualifying scores.

An aggregate model that accurately approximates the dynamics of compressor-based TCLs under PEM is yet to be developed. The existing macro-models described in the introduction do not account for compressor-based loads like ACs under PEM control. Such a model is important to analytically ascertain the flexibility limits of a fleet of compressor-based TCLs under PEM. An aggregate model is also vital for analytically determining the population steady-state distribution and analyzing dynamic behavior. Additionally, it would allow sensitivity analysis and optimal design of parameters such as epoch and mean request frequencies.

The PEM scheme requires bi-directional communication links between devices and the aggregator compared to some other schemes that employ unidirectional message broadcasting. Future work will explore controller characteristics and performance in the presence of communication latency and drop-outs, and will develop strategies to mitigate issues associated with these real-world challenges. We will also consider ways of enhancing the PEM controller to achieve distribution-network awareness. Furthermore, we will benchmark PEM against other state-of-the-art control strategies to understand trade-offs between centralized methods and more distributed schemes like model-free PEM.

## Acknowledgment

We thank Duncan Callaway, Phillippe Phanivong, Ioannis Granitsas, Adil Khurram, and the teams at Pecan Street and Packetized Energy for stimulating conversations.

## References

[1] J. A. Taylor, S. V. Dhople, and D. S. Callaway, "Power systems without fuel," *Renewable and Sustainable Energy Reviews*, vol. 57, pp. 1322–1336, 2016.

[2] F. Schweppe, R. Tabors, J. Kirtley, H. Outhred, F. Pickel, and A. Cox, "Homeostatic utility control," *IEEE Trans Power Apparatus and Systems*, vol. PAS-99, pp. 1151–1163, May 1980.

[3] Y. Ding, Y. Song, H. Hui, and C. Shao, *Integration of Air Conditioning and Heating into Modern Power Systems*. Springer, 2019.

[4] D. S. Callaway, "Tapping the energy storage potential in electric loads to deliver load following and regulation, with application to wind energy," *Energy Conversion and Management*, vol. 50, no. 5, pp. 1389–1400, 2009.

[5] D. S. Callaway and I. A. Hiskens, "Achieving controllability of electric loads," *Proceedings of the IEEE*, vol. 99, no. 1, pp. 184–199, 2011.

[6] J. L. Mathieu, S. Koch, and D. S. Callaway, "State estimation and control of electric loads to manage real-time energy imbalance," *IEEE Trans Power Systems*, vol. 28, no. 1, pp. 430–440, 2013.

[7] A. Nayyar, J. Taylor, A. Subramanian, K. Poolla, and P. Varaiya, "Aggregate flexibility of a collection of loads," *IEEE Conference on Decision and Control*, pp. 5600–5607, 2013.

[8] H. Hao, B. M. Sanandaji, K. Poolla, and T. L. Vincent, "Aggregate flexibility of thermostatically controlled loads," *IEEE Trans Power Systems*, vol. 30, no. 1, pp. 189–198, 2015.

[9] Federal Energy Regulatory Commission, "FERC Order No. 2222: Fact Sheet." `https://www.ferc.gov/media/ferc-order-no-2222-fact-sheet`, 2020.

[10] U.S. Energy Information Administration, "Table CE3.1 Annual household site end-use consumption in the U.S. 2015." `https://www.eia.gov/consumption/residential/data/2015/c&e/pdf/ce3.1.pdf`, 2015.

[11] L. W. Davis and P. J. Gertler, "Contribution of air conditioning adoption to future energy use under global warming," *Proceedings of the National Academy of Sciences*, vol. 112, no. 19, pp. 5962–5967, 2015.

[12] M. Izquierdo, A. Moreno-Rodríguez, A. González-Gil, and N. García-Hernando, "Air conditioning in the region of Madrid, Spain: An approach to electricity consumption, economics and CO2 emissions," *Energy*, vol. 36, no. 3, pp. 1630–1639, 2011.

[13] A. D. Dominguez-Garcia, S. T. Cady, and C. N. Hadjicostis, "Decentralized optimal dispatch of distributed energy resources," *IEEE Conference on Decision and Control*, pp. 3688–3693, 2012.

[14] S. Koch, *Demand response methods for ancillary services and renewable energy integration in electric power systems*. PhD thesis, ETH Zurich, 2013.

[15] C. Perfumo, J. H. Braslavsky, and J. K. Ward, "Model-based estimation of energy savings in load control events for thermostatically controlled loads," *IEEE Trans Smart Grid*, vol. 5, no. 3, pp. 1410–1420, 2014.

[16] S. Grammatico, B. Gentile, F. Parise, and J. Lygeros, "A mean field control approach for demand side management of large populations of thermostatically controlled loads," in *2015 European Control Conference (ECC)*, pp. 3548–3553, 2015.

[17] D. Wu, J. Lian, Y. Sun, T. Yang, and J. Hansen, "Hierarchical control framework for integrated coordination between distributed energy resources and demand response," *Electric Power Systems Research*, vol. 150, pp. 45–54, sep 2017.

[18] B. Chen, J. Francis, M. Pritoni, S. Kar, and M. Bergés, "COHORT: Coordination of Heterogeneous Thermostatically Controlled Loads for Demand Flexibility," *BuildSys - ACM International Conference on Systems for Energy-Efficient Buildings, Cities, and Transportation*, pp. 31–40, nov 2020.

[19] M. Franceschelli, A. Pilloni, and A. Gasparri, "Multi-Agent Coordination of Thermostatically Controlled Loads by Smart Power Sockets for Electric Demand Side Management," *IEEE Trans Control Systems Technology*, vol. 29, no. 2, pp. 731–743, 2021.

[20] K. Kircher, A. Aderibole, L. K. Norford, and S. Leeb, "Distributed Peak Shaving for Small Aggregations of Cyclic Loads," *IEEE Trans Power Delivery*, vol. 8977, no. c, pp. 1–1, 2022.

[21] M. Almassalkhi, J. Frolik, and P. Hines, "Packetized energy management: Asynchronous and anonymous coordination of thermostatically controlled loads," *American Control Conference*, 2017.

[22] M. Almassalkhi, L. Duffaut-Espinosa, P. Hines, J. Frolik, S. Paudyal, and M. Amini, "Asynchronous coordination of distributed energy resources with packetized energy management," in *Energy Markets and Responsive Grids* (S. Meyn, T. Samad, I. Hiskens and J. Stoustrup, ed.), Springer, 2018.

[23] L. A. Espinosa, M. Almassalkhi, P. Hines, and J. Frolik, "Aggregate modeling and coordination of diverse energy resources under packetized energy management," *IEEE Conference on Decision and Control*, pp. 1394–1400, 2018.

[24] L. A. Espinosa, M. Almassalkhi, P. Hines, and J. Frolik, "System properties of packetized energy management for aggregated diverse resources," *Power Systems Computation Conference*, 2018.

[25] L. A. D. Espinosa and M. Almassalkhi, "A Packetized Energy Management Macromodel With Quality of Service Guarantees for Demand-Side Resources," *IEEE Trans Power Systems*, vol. 35, no. 5, pp. 3660–3670, 2020.

[26] L. A. Espinosa, A. Khurram, and M. Almassalkhi, "Reference-Tracking Control Policies for Packetized Coordination of Heterogeneous DER Populations," *IEEE Trans Control Systems Technology*, 2020.

[27] H. Mavalizadeh, L. A. Duffaut Espinosa, and M. R. Almassalkhi, "Decentralized frequency control using packet-based energy coordination," *IEEE SmartGridComm*, 2020.

[28] C. Y. Chang, W. Zhang, J. Lian, and K. Kalsi, "Modeling and control of aggregated air conditioning loads under realistic conditions," *Innovative Smart Grid Technologies Conference*, 2013.

[29] "Tech:Residential – GridLAB-D Wiki." `http://gridlab-d.shoutwiki.com/wiki/Tech:Residential`.

[30] R. Pratt and Z. Taylor, "Development and testing of an equivalent thermal parameter model of commercial buildings from time-series end-use data." Pacific Northwest National Laboratory, 1994.

[31] R. Sonderegger, "Dynamic models of house heating based on equivalent thermal parameters." Princeton University, 1978.

[32] K. Subbarao, "Thermal parameters for single and multizone buildings and their determination from performance data." Solar Energy Research Institute, 1981.

[33] N. Wilson, B. Wagner, and W. Colborne, "Equivalent thermal parameters for an occupied gas-heated house," *ASHRAE Transactions*, vol. 91, p. 2, 1985.

[34] W. Zhang, K. Kalsi, J. Fuller, M. Elizondo, and D. Chassin, "Aggregate model for heterogeneous thermostatically controlled loads with demand response," *IEEE Power & Energy Society General Meeting*, 2012.

[35] PJM Interconnection, "PJM - Ancillary Services." `https://pjm.com/markets-and-operations/ancillary-services`.

[36] CPowerEnergyManagement, "How the PJM interconnection frequency regulation program works." `https://cpowerenergymanagement.com/wp-content/uploads/2019/03/PJM_FR_Snapshot_3-1-2019.pdf`, 2019.

[37] A. Khurram, L. Duffaut Espinosa, and M. Almassalkhi, "A Methodology for Quantifying Flexibility in a fleet of Diverse DERs," in *IEEE PES PowerTech*, 2021.